Influence of defect pairs in Ga-based ordered defect compounds: A hybrid density functional study

Sudhir Kumar[1],* Suman Joshi[1,2], Durgesh Kumar Sharma[1], and Sushil Auluck[3]
[1] *Applied Physics Department, Faculty of Engineering and Technology, M. J. P. Rohilkhand University, Bareilly - 243 006, India*
[2] *Physics Department, Rajshree Institute of Management and Technology, Bareilly - 243 122 , India*
[3] *CSIR-National Physical Laboratory, Dr K. S. Krishnan Marg, New Delhi - 110 012, India*
(Dated: October 23, 2019)

In the present paper, density functional theory (DFT) based calculations have been performed in order to predict the stability, electronic and optical properties of Ga-rich ordered defect compounds (ODCs). The calculated lattice constants, bulk modulus, their pressure derivatives and optical constants show good agreement with available experimental data. The hybrid exchange correlations functional have been considered to calculate ground state total energy and energy band gap of the material. The calculated formation energy of ODCs comes smaller than pure $CuGaSe_2$ (CGS). Our calculated optical absorption coefficients indicate that the energy band gap of ODCs can be tuned by changing the number of donor-acceptor defect pairs ($2V_{Cu}^{-} + Ga_{Cu}^{2+}$). The band offset has been calculated to understand the reason of band gap alteration while number of defect pair changes. Our results may be helpful for experimentalist to further improve the performance of ODCs.

PACS numbers: 35.15.E-, 71.20.-b,71.20.Nr, 78.20.-e, 85.30.-z

I. INTRODUCTION

In order to meet the ever increasing demand of energy in the form of electricity while keeping the environment clean, photovoltaic technology has potential and emerged as a useful and competitive source to produce electricity by utilizing solar energy. In recent years, the CGS based materials have been considered to be among the most promising high efficiency thin film solar cells due to mainly its high optical absorption [1]. CGS exists in tetragonal structure with a space group I42d, consists 16 atoms in a unit cell. The formation of defect and defect phases affects the micro-structural, electrical and optical properties of $Cu(In,Ga)Se_2$ (CIGS) film including the solar cell performance [2]. The quaternary CIGS which is a pseudo-binary compound of $CuInSe_2$ (CIS) and CGS with the band gap energy lying between 1.04 to 1.64 eV can be tuned by varying Ga amount [3]. Wooley *et al*. [4] measured valence to conduction band transition energies for $CuGa(S_{1-z}Se_z)_2$ as a function of temperature. They also discussed role of *p-d* hybridization on spin orbit and crystal field splitting using theoretical model. A. Ennaoui [5] developed $Cu(Ga,In)(S,Se)_2$ (CIGSS)/ZnSe hetrojunction Cd-free thin films chalcopyrite which shows 13.7% efficiency with 10 nm thickness of ZnSe. He also measured valence and conduction band offset equal to 0.60 and 1.27 eV, respectively by using x-ray photoemission spectroscopy. Nevertheless, the correlation with material properties, defects and their impact on the device performance are indispensable to achieve power conversion efficiency beyond the current limit. The band gap may be increased either by replacing Ga by Al or forming a series of Cu deficient ODCs. In this paper, we have chosen the second option *i.e*. the number of defect pairs ($2V_{Cu}^{-}$ + Ga_{Cu}^{2+}) in each compound are equal to the number of unit cells of the respective compound.

The energy band gap of ODCs can be varied with the number of defect pairs, more importantly without much change in lattice constants (≈5%). This provides great flexibility to tune the band gap for specific application such as tandem solar cells. Recently, Yani-Albe [6] presented a detailed study for CIS and CGS compounds. Their study mainly devoted to dislocations and discussion about the formation of dangling bond states. Alonso *et al*. [7] have grown Cu-III-VI_2 (III = Ga, In and VI = S, Se) compounds by using iodine vapor transitions and measure the complex dielectric function components within the energy range of 1-5 eV. Moreover, the optical constants of $Cu_2In_4Se_7$ and $CuGa_3Se_5$ compounds have been measured by Leon *et al* [8]. In another work of Leon *et al*. [9], $Cu_2In_4Se_7$, $CuGa_3Se_5$ and $CuGa_5Se_8$ compounds have been successfully grown at room temperature. By using the ellipsometry technique they have investigated the optical response. Similarly, a detailed investigation of the optical constants has been performed by Duran *et al*. [10] for ODCs like $CuGa_5Se_8$ and $CuIn_5Se_8$. To find the energy gap they have fitted the experimental data to the second derivative of optical properties (absorption, dielectric function, etc). Grossberg *et al*. [11] have studied the photoluminescence and Raman properties of $CuGa_5Se_8$ crystal. There seems to be a dearth of theoretical work to get deep insight into the structural, electronic and optical properties of ODCs.

Looking into the above available details, we motivated to predict influence of donors-acceptor defect pair ($2V_{Cu}^{-}$ + Ga_{Cu}^{2+}) concentration on (i) structural parameters and stability of defected system, (ii) deviation in band edges and energy band gaps, and (iii) variation in optical absorption spectra of defected systems. To explore these properties, a series of first principles calculations based of

* skumar@mjpru.ac.in; drsudhirkumar.in@gmail.com

DFT, using appropriate exchange correlation functional, have been carried out. The computational details for solving Kohn-Sham equations have been discussed in sec. II. However, based on calculations obtained results and discussion have been presented in sec. III. Finally, on the basis of results and discussion, we concluded our predictions in sec. IV.

II. COMPUTATIONAL DETAILS

The DFT based calculations have been carried out by using the Vienna Ab-initio Simulation Package (VASP) [12]. VASP uses the projector augmented wave method [13] to define the interaction between core and valence electrons. For valence electrons, we consider Cu($3d^{10}$, $4s^1$), Ga($3d^{10}$, $4s^2$, $4p^1$), and Se($4s^2$, $4p^4$) electrons in valence states while remaining were assumed inside the frozen core. To expand plane wave basis sets, fixed kinetic energy cut off equal to 300 eV has been chosen for all the calculations. However, different k-points mesh has been set for different purposes. For the density of states calculations, the Monkhorst-Pack [14] k-points mesh of size 4×4×4 has been used. However, a dense mesh of 6×6×6 has been set to calculate optical properties. These input parameters have been tested with respect to plane wave cut off energy and k-points mesh. The deviation in total energy with higher values of these parameters is about 0.1 meV which does not affect our results significantly. The energy convergence threshold between two consecutive iterations has been set upto 10^{-6} eV. The Gaussian broadening (σ) is taken to be 0.05 eV for all calculations. We relax each atom until the Hellmann-Feynman force on atoms becomes less than 0.01 eV/Å.

Defect calculations based on DFT, within local density approximation (LDA) [15] or generalized gradient approximation (GGA) [16], have been hampered by the underestimation of energy band gap. The on-site Coulomb term in LDA/GGA+U approach partially resolve the band gap problem. However, the hybrid functional as proposed by Heyd-Scuseria-Ernzerhof (HSE06) [17, 18] is able to reproduce the experimental energy band gap reasonable well [19, 20]. The hybrid functional is becoming a popular method for getting reliable results for electronic structure of solids [21, 22]. In HSE06, the amount of Hartree-Fock exchange mixing parameter (α) gives the strength of the non-local exchange and ω represents screening parameter that controls the spatial range where the non-local exchange part is important. The choice of α and ω may depend on the actual system. We have fixed the parameter ω=0.2 a_0^{-1} while varied α and set equal to 0.33. Thus, we call our calculations HSE instead of HSE06. To predict structure stability, electronic band structure and density of states, we have used HSE hybrid density functional.

III. RESULTS AND DISCUSSION

A. Structural properties and stability

We have used van der Waals (vdW) density functional (DF) to determine the structural parameters of Ga based bulk and defected chalcopyrite semiconductors. This represents the local atom bonds and weak vdW forces between atoms in layered structure compounds correctly. However, standard LDA or GGA fail to describe the interaction for the sparse electron density. The vdW-DF method is very appealing since it is directly based on the electron density and takes the form of

$$E_{xc} = E_x^{GGA} + E_c^{LDA} + E_c^{nl} \quad (1)$$

where the exchange energy E_x^{GGA} uses the PBE functional [16] while E_c^{LDA} incorporates the LDA [15] functional based correlation energy. The term E_c^{nl} denotes the nonlocal energy contribution which accounts the nonlocal electron correlation effect. The nonlocal energy is obtained by doing a double space integration which gives an improved structural parameters compared to local or semi local functional. The nonlocal correlations are thought to be more important where core electron densities have relatively large polarizability as in the case of Cu [23]. Using the efficient implementation of vdW-DF by Román-Pérez and Soler [24], a self consistent field calculation takes about the same time as the standard LDA/GGA.

The optimized crystal parameters are obtained by minimizing the total energy for set of volumes of a unit cell and c/a ratio. Further, the equilibrium volume and c/a ratio were calculated by using the Murnaghan equation of state [25]. The anion displacement parameter (u) is obtained by using the Abrahams and Bernstein [26] formula which relates u and tetragonal distortion η = c/2a as follows:

$$u = \frac{1}{2} - \frac{1}{4}\sqrt{2\eta^2 - 1} \quad (2)$$

The predicted lattice parameters are presented in Table I along with the available measured data. The optimized lattice constants give much improved results compared to LDA/GGA with an average error of ≈ 2%. This agreement strongly depends on the core electron density which shows relatively large deviation in the ODCs. Overall, our calculation shows smaller value than the experimental data of structural parameters. The calculated lattice constant (a) shows similar trend after introducing defect pair contrary to c/a ratio.

The bulk modulus and its pressure derivatives are also calculated by fitting the fourth-order Murnaghan equation of state [33] and found to be 76.31 GPa and 4.47 for CGS. The calculated bulk modulus of CGS is in good agreement with available experimental values of 75.67 [32], 70.18 [34] and 69.31 GPa [35]. However, there is no experimental data available for pressure derivates, presented in Table I.

TABLE I. The calculated lattice constants (in Å) and energy band gap (in eV) for CGS, $CuGa_5Se_8$ and $CuGa_3Se_5$ ODCs, along with the bulk modulus B (in GPa) and its derivative B$^{'}$ for CGS.

System	$CuGaSe_2$	$CuGa_5Se_8$	$CuGa_3Se_5$
Present Work:			
a	5.5516	5.4114	5.4197
c/a	1.9573	1.9893	1.9850
u	0.2607	0.2526	0.2537
η	0.9786	0.9946	0.9925
B	76.31	-	-
B$^{'}$	4.4714	-	-
E_g	1.67	1.80	1.78
Experimental:			
a	5.610[27]	5.481[28]	5.498[29]
	5.596[30]	5.473[31]	5.499[31]
c/a	1.96	1.99	1.98
	1.96	1.99	1.99
u	0.2601	0.2510	0.2520
	0.2668	0.2500	0.2525
η	0.980	0.997	0.994
	0.983	0.998	0.995
B	75.67[32]	-	-
B$^{'}$	-	-	-
E_g	1.68[27]	1.92[9]	1.78-1.87[9]

The ODCs like $CuGa_5Se_8$ and $CuGa_3Se_5$ may be the future materials having application in the area of high efficiency thin film solar cells. These can be obtained by a perfect CGS with a defect pair ($2V_{Cu}^{-}$+Ga_{Cu}^{2+}). One can generate $CuGa_5Se_8$ and $CuGa_3Se_5$ by considering 4 and 5 unit cells along [100] direction which consists 64 and 80 atoms in the supercell. Ga-rich (Cu-poor) compounds are formed by the following reaction [36]:

$$n(CuGaSe_2) + m(Ga) \longrightarrow Cu_{(n-3m)}Ga_{(n+m)}Se_{2n} + 3m(Cu) + E_f(n,m) \quad (3)$$

where n = 4, 5, 7, ... are the number of unit cell of CGS and $m = 1$ represents the number of defect pairs i.e. ($2V_{Cu}^{-} + Ga_{Cu}^{2+}$) in each CGS unit cell. In the above equation (Ga) and (Cu) denotes Ga and Cu in respective equilibrium chemical reservoirs. The energy $E_f(n,m)$ needs to form defect pair arrays from CGS which is very close to zero. However, to get deep insights about $E_f(n,m)$, one can cite the paper of Zhang *et al* [36]. The calculated low formation energy informs about the existence of $CuGa_5Se_8$ and $CuGa_3Se_5$ as repeated ($2V_{Cu}^{-} + Ga_{Cu}^{2+}$) in single unit for n = 4 and 5, respectively [37].

We now address the stability of ODCs, resulting from the repetition of m units of ($2V_{Cu}^{-} + Ga_{Cu}^{2+}$) for every n unit of CGS. These are $CuGa_5Se_8$ ($n = 4$, $m = 1$) and $CuGa_3Se_5$ ($n = 5$, $m = 1$). The crystal structure of $CuGa_5Se_8$ defect chalcopyrite with four defect pair is shown in Fig. 1.

The stability of defective system can be determined by knowing the formation energy (E_f) which can be calculated by equation as given below:

$$E_f = E(CuGaSe_2) - E(Cu) - E(Ga) - 2E(Se) \quad (4)$$

where $E(CuGaSe_2)$ represents the total energy per atom of CGS while $E(Cu)$, $E(Ga)$ and $E(Se)$ are the total energies of Cu, Ga and Se in an isolated form. The calculated values of formation energy are equals to -3.78, -3.86, -4.04 eV for CGS, $CuGa_5Se_8$ and $CuGa_3Se_5$, respectively. Our calculation shows that E_f decreases from n = 4 to 5 which confirms that the tetragonal phase ODCs are stable.

B. Band structure

The electronic band structure of CGS and $CuGa_5Se_8$ are shown in Fig. 2(a) and 2(b), respectively having direct energy band gap at the Γ point. We have presented band structure along T (0,0,1), Γ (0,0,0) and N (1,1,0) symmetry line in Fig. 2. The calculated energy band gap using the HSE functional depends on the parameter α. For $\alpha = 0.33$, we obtained (measured) energy band gap for CGS, $CuGa_5Se_8$ and $CuGa_3Se_5$ equals to 1.67 (1.68), 1.80 (1.92-1.97) and 1.78 (1.78-1.87) eV, respectively, presented in Table I. Our calculated values of energy band gaps are in good agreement with the available measured data. We find that HSE corrects the energy band gap by pushing down (up) the valence (conduction) band compared to GGA [16]. As shown in Fig. 2(a) and 2(b), the VBM is mainly composed by Cu-3d bands having flat character up to $\sim$ 7 eV below of VBM. The conduction band minimum (CBM) derived mainly from Ga-4s orbital. Further, by introducing the defect pair ($2V_{Cu}^{-}$ + Ga_{Cu}^{2+}) in pristine CGS, the band width of Cu-3d bands decrease by 1 eV. On the other hand, Se-4p states become more delocalized in the lower valence band while Ga-4s states still dominated in the CBM. By further increasing the defect pair in $CuGa_3Se_3$, no significant changes have been seen in VBM and CBM regions.

C. Band offsets

When two semiconductors are in contact with each other, their energy bands as well as wave functions at the interface region get influenced. The wave functions decay exponentially from one material into other, resulting a complex band structure formed [38]. At a certain energy, called branch point energy (E_{BP}), the states change their character from valence to conduction bands like from one material to other. Such states transfer a net charge, the sign of which depends on the position of E_{BP}. The electronic structure calculations give energy eigenvalue at each desired k-point of the Brillouin zone.

We have calculated E_{BP} by averaging the eigenvalues of the two highest valence bands and two lowest conduction bands as reported previously [39]. The E_{BP} is

defined by:

$$E_{BP} = \frac{1}{2N_k}\sum_{k}\left[\frac{1}{N_{CB}}\sum_{i}^{N_{CB}}\varepsilon_{c_i}(k) + \frac{1}{N_{VB}}\sum_{j}^{N_{VB}}\varepsilon_{v_j}(k)\right] \quad (5)$$

where N_k is number of k-points incorporated during calculations while N_{CB} and N_{VB} are the number of valence and conduction bands. We have chosen $N_{CB} = 2$ and $N_{VB} = 2$. Those band which shows minimum dispersion has to be included. The E_{BP} alignment at the band edges for CGS and its ODCs lead to the band edges with respect to conduction (E_c) and valence (E_v) edge and consequently the band discontinuation ΔE_v and ΔE_c has been provided, as presented in Fig. 3. The VBM of CGS has a value (-0.6584 eV) compared to other defect compounds $CuGa_5Se_8$ (-0.732902 eV) and $CuGa_3Se_5$ (-0.642575 eV), respectively. On the other hand, the value of CBM increases on increasing the number of unit cell. Hence the increase in the band gap of ODCs is mainly due to change in CBM. The rising of CBM is due to the combined effect of Cu vacancies and Ga_{Cu} antisites. It is relatively small because the effective electrostatic potential of the vacancies and antisites have opposite sign, thus, cancels out each other. This band alignment between Cu-poor ODCs and CGS could have a significant effect on the solar cell performance [40]. This suggests that the change in VBM is within 10 %. On the other hand, CBM increases monotonously. The details of the states, dominated by constituent atoms at the interface, are discussed in section 3.4. However, the CIGSS/ZnSe hetrojunction shows that ΔE_v and ΔE_c are equals to 0.60 and 1.27 eV, respectively [5].

D. Density of States

The value of energy band gaps slightly increases with increase of number of defect pairs because of the blue shift of Ga-4s states which are strongly hybridized with Se-4s states. The anion displacement parameter undoubtedly has a large impact on the electronic structure and decreases slightly with increase in defect pair that may also lead to a slightly smaller energy band gap.

We present the total density of states (DOS) in Fig. 4 (left) and partial DOS in Fig. 4 (right) for CGS, $CuGa_5Se_8$ and $CuGa_3Se_5$. The valence band can be divided into three regions. The bands at the lowest energy region (below -13 eV from the VBM) which we call VB_1, are mainly contributed by a strong hybridization between Se-4s and Ga-4s states with small contribution of Ga-4p states. The band width of VB_1 is around 2.38 eV. With the addition of a defect pair, the width of the VB_1 increases and reaches to a maximum value of 6.64 eV for $n = 5$ ($CuGa_3Se_5$). Singlet structure below -13 eV split into multiple structures, dominated mainly by two states at -14.30 and -15.22 eV. This occurs due to the strong hybridization between Se-4s and Ga-4s states. The structure in the intermediate energy region (located between -6.0 to -9.0 eV which we call VB_2) is basically formed by Ga-4s and Se-4p states hybridization. The intermediate structure merge in VB_3 with increasing number of defect pairs i.e. $n = 4$. The states around 0 to -5.0 eV in the valence band which we call VB_3, are mainly contributed by Cu-3d and Se-4p states. The noticeable contribution to VBM from Ga-4p and Cu-p states has been predicted. The results from the partial DOS analysis are in good agreement with the previous ab-initio calculations [41]. The position, dispersion and character of the lowest conduction band carry the key features and are responsible for the optical properties. The CBM of CGS and ODC are mainly originated by Ga-4s states with a small contribution from Ga-4p and Se-4p and site decomposed DOS analysis is used for the details characterization of the contribution of electrons.

As we have discussed above, there are three regions in the valence bands, considered in the present work for CGS and ODCs. According to DOS analysis, VB_2 and VB_3 merge to make a wider valence band width of 9.29 eV for $CuGa_5Se_8$. On further increase in the number of defect pairs ($2V_{Cu}^{-} + Ga_{Cu}^{2+}$), it increases slightly and becomes equal to 9.32 eV for $CuGa_3Se_5$. Analysis shows that with increasing defect pairs ($2V_{Cu}^{-} + Ga_{Cu}^{2+}$), valence band width increases i.e. VB_1 & VB_2, results electrons get more delocalized.

E. Optical Properties

The dielectric functions $\varepsilon(\omega) = \varepsilon_1(\omega) + i\varepsilon_2(\omega)$ can be calculated by considering direct transitions from occupied to unoccupied states. The investigated crystals have tetragonal symmetry therefore, one needs to calculate two components of dielectric tensor. These are representing electric field (E) perpendicular and parallel to the optical c-axis, known as the ordinary ($\varepsilon_2^{xx}(\omega) = \varepsilon_2^{yy}(\omega) = \varepsilon_2^{\perp}(\omega)$) and extraordinary ($\varepsilon_2^{zz}(\omega) = \varepsilon_2^{||}(\omega)$) dielectric function corresponding to $E \perp c$ and $E \| c$, respectively. The imaginary part of the dielectric function was calculated by using the expression:

$$\varepsilon_2(\omega) = \frac{4\pi^2 e^2}{\Omega} lim_{q\longrightarrow 0}\frac{1}{q^2}\sum_{c,v,k} 2\omega_k \delta[\varepsilon_{ck} - \varepsilon_{vk} - \omega) \times < u_{ck} + e_{\alpha q}|u_{vk} >< u_{ck} + e_{\beta q}|u_{vk} > \quad (6)$$

where the indices c and v refer to conduction and valence band states, respectively and u_{ck} is the cell periodic part of the wave functions at the k-point. The real part of the dielectric function can be obtained by using Kramer-Kronig transformation:

$$\varepsilon_1(\omega) = 1 + \frac{2}{\pi} P\int_0^{\infty}\frac{\varepsilon_2(\omega)\omega'}{\omega'^2 - \omega^2 + i\eta} d\omega' \quad (7)$$

where P denotes the Cauchy principal value. The method is explained in details by Gajdos *et al* [42]. However, more detailed calculation for optical constants are explained elsewhere in Ref. [43]. The optical properties

TABLE II. The calculated peak position of imaginary part of dielectric function $\varepsilon_2(\omega)$ for E⊥c (E∥c).

System	$CuGaSe_2$	$CuGa_5Se_8$	$CuGa_3Se_5$
$T_1(P_1)$	2.15(1.98)	2.15(-)	2.15(-)
$T_2(P_2)$	3.91(3.86)	3.9(3.86)	3.91(3.86)
$T_3(P_3)$	5.70(5.67)	5.70(-)	5.70(-)
$T_4(P_4)$	6.67(7.52)	-(6.4)	6.67(7.52)
$T_5(P_5)$	7.49(-)	7.44(8.0)	-

TABLE III. The calculated peak position of real part of dielectric function $\varepsilon_1(\omega)$ for E⊥c (E∥c).

System	$CuGaSe_2$	$CuGa_5Se_8$	$CuGa_3Se_5$
$R_1(S_1)$	3.14(3.0)	2.85(3.02)	2.79(2.98)
$R_2(S_2)$	3.34(4.59)	4.87(4.52)	4.89(4.46)
$R_3(S_3)$	6.18(6.46)	-	-
$R_4(S_4)$	8.24(-)	8.34(-)	8.38(-)

of the ODCs provide the basis for a vast range of investigations. Therefore, it is important to describe accurately such properties by efficient ab-initio approach. The calculated spectra for imaginary part of the dielectric function i.e. ordinary (left) E⊥c and extraordinary (right) E∥c for CGS, $CuGa_5Se_8$ and $CuGa_3Se_5$ are presented in Fig. 5(a-f). We have also included the corresponding measured experimental data [7, 8, 10] for shake of comparison. The experimental data are extended up to 5 eV for the ordinary and extraordinary tensor component of the dielectric function. There is common a feature to all spectra. At first, threshold of the calculated dielectric function corresponds to a transition at Γ point which is equal to the energy band gap. Our calculated onset energies are 1.67, 1.80 and 1.78 eV (underestimated by 0.5% to 6.0% of the measured value). The peak position in Fig. 5(a-c) is different for different materials. For the perfect CGS there are five peaks at 2.15(T_1), 3.91(T_2), 5.70(T_3), 6.67(T_4), 7.49(T_5) eV. The first two peaks T_1 and T_2 are mainly due to the transition from Cu-3d and Se-4p states from the valence to conduction bands at Γ point. The peaks T_3 and T_4 corresponds to the transition from Se-4p and Ga-4s states of valence band to the second highest conduction bands. The peaks T_5 may appear as an almost dispersion less group of bands, separated by small gaps from the above and below to the Fermi energy. We have predicted that the transitions from these levels are above 3 eV in the absorption spectra. For $CuGa_5Se_8$, the T_3, T_4 and T_5 peaks merged as a single peak as T_5 at 6.46 eV, shown in Fig. 5b. The non degenerate different states of the Cu, Ga and Se are closer causing a broad structure with increasing n. However, the position of T_1 and T_2 remains the same in Fig. 5(a-c). The extraordinary dielectric function presented in Fig. 5(d-f) which shows five structures P_1(1.98), P_2(3.86), P_3(5.67), P_4(7.52) and P_5(8.28) for CGS. There is a shoulder P_5(8.28) which appears at higher energy due to the transition from lowest VB_3 bands to the higher energy in conduction bands, mainly at Γ symmetry point in CGS. Further, with increasing n the P_5 shoulder move towards lower energy and finally it disappears for $CuGa_3Se_5$. On the other hand, P_1 peak moves toward the higher energy and merge into P_2. The P_3 and P_4 peaks merge into a single broad structure at 6.53 eV into P_4, presented in Fig. 5(d-f). The measured spectra for CGS presented in inset of Fig. 5(a), shows two peaks with a bump at 2 eV which is similar to the calculated one except the red shift. Additionally, the spectra for $CuGa_5Se_8$ and $CuGa_3Se_5$ are featureless similar to the measured spectra presented in inset Fig. 5(b and c). Further, from the above spectra, we have also predicted that the amplitudes of the optical transitions for ODC are always smaller than those of parent compounds. This is in accord with the reduced DOS near VBM due to Cu-deficiency. All the peak positions of $\varepsilon_2(\omega)$ for E⊥c (E∥c) have been summarized in Table II.

Moreover, the static dielectric constant $\varepsilon_1(0)$ strongly depends on the energy band gap. The precise determination of $\varepsilon_1(0)$ is complicated because of the known fact that LDA/GGA underestimates energy band gaps. Thus our calculated static dielectric constant (measured) for CGS, $CuGa_5Se_8$ and $CuGa_3Se_5$ are equal to 13.57 (8.16), 10.37 (7.05) and 8.64 (7.29) eV larger than the measured experimental data [7, 8, 10], presented in Fig. 6(a-f). The peak positions of real part of the dielectric function $\varepsilon_1(\omega)$ for E⊥c (E∥c) are presented in Table III.

IV. CONCLUSION

We have reported a systematic study of the influence of defect pairs ($2V^{-}_{Cu}$ + Ga^{2+}_{Cu}) on the structural, electronic and optical properties of CGS and ODCs. The calculated lattice constants show very similar trend as observed in the available experimental data. To describe the stability of defect compounds, we have calculated the formation energy which is small and negative. Thus, exothermic chemical reaction is possible. The calculated energy band gap for the perfect ternary semiconductor CGS and their ODCs are direct which is consistent with the earlier reports. The calculated energy band gap of ODCs is larger than the bulk CGS. We have also discussed the valence band offset which suggest that the ODCs may be p-type material. We discuss the relations of the peaks of the dielectric function with the inter band transitions in detail. There is a reduction in the DOS of Cu-3d states near the VBM because one of the Cu atom is replaced by Ga atom. The effect of reduced DOS results in a decrease in the amplitudes of the absorption coefficient of ODCs. The partial DOS explain the character of contributed orbital. The present results offer the valuable optical data for parent CGS as well as for its ODCs. Our work could serve as a good reference for future optical applications of the CGS based photovoltaic solar cells.

V. ACKNOWLEDGEMENTS

This work was supported by the Department of Science and Technology (DST) and Defence Research and Development Organization (DRDO), New Delhi, India. SA would like to acknowledge the use of the High Performance Computing (HPC) facilities at Physics Department of Indian Institute of Technology in Kanpur (IITK), Intra-University Accelerator Centre (IUAC) in New Delhi, Institute of Mathematical Sciences (IMSc) in Chennai, Council of Scientific and Industrial Research Fourth Paradigm Institute (CSIR-4PI) at Bangaluru and University of Hyderabad in Hyderabad.

[1] I. Repins, M. A. Contreras, B. Egaas, C. DeHart, J. Scharf, C. L. Perkins, and R. To, B. Noufi, Prog. in Photovoltaics: Research and Applications **16**, 235 (2008).
[2] M. M. Islam, T. Sakurai, S. Ishizuka, A. Yamada, H. Shibata, K. Sakurai, K. Matsubara, N. S., and K. Akimoto, Journal of Crystal Growth **311**, 2212 (2009).
[3] S. Ishizuka, A. Yamada, P. J. Fons, H. Shibata, and S. Niki, Prog. in Photovoltaics: Research and Applications **22**, 821 (2014).
[4] M. Quintero, K. Yoodee, and J. C. Woolley, Can. J. Phys. **64(1)**, 45 (1986).
[5] A. Ennaoui, Can. J. Phys. **77(9)**, 723 (2000).
[6] D. B. Yani and K. Albe, Phys. Rev. B **95**, 115203 (2017).
[7] M. I. Alonso, K. Wakita, J. Pascual, M. Garriga, and N. Yamamoto, Phys. Rev. B **63**, 2001 (075203).
[8] M. Leon, R. Serna, S. Levcenko, A. Nateprov, A. Nicorici, J. M. Merino, and A. E., J. Appl. Phy. **101**, 013524 (2007).
[9] M. Leon, S. Levcenko, A. Nateprov, A. Nicorici, J. M. Merino, R. Serna, and E. Arushanov, J. Phys. D. **40**, 740 (2007).
[10] L. Duran, J. Castro, J. Naranjo, J. R. Fermin, and C. A. Durante Rincon, Materials Chemistry and Physics **114**, 73 (2009).
[11] M. Grossberg, J. Krustok, I. Bodbar, S. Siebentritt, and J. Albert, Physica B **403**, 184 (2008).
[12] G. Kresse and J. Furthmuller, Comp. Mat. Sci. **6**, 15 (1996).
[13] P. E. Blochl, Phys. Rev. B **50**, 17953 (1994).
[14] H. J. Monkhorst and J. D. Pack, Phys. Rev. B **13**, 5188 (1976).
[15] D. Ceperley and B. Alder, Phys. Rev. Lett. **45**, 566 (1980).
[16] J. P. Perdew, K. Burke, and M. Ernzerhof, Phys. Rev. Lett. **77**, 3865 (1996).
[17] J. Heyd, G. E. Scuseria, and M. Ernzerhof, J. Chem. Phys **118**, 8207 (2003).
[18] J. Heyd, G. E. Scuseria, and M. Ernzerhof, J. Chem. Phys. **124**, 219906 (2006).
[19] S. Kumar, D. K. Sharma, and S. Auluck, Phys. Rev. B **94**, 235206 (2016).
[20] S. Kumar, D. K. Sharma, B. Joshi, and S. Auluck, AIP Adv. **6**, 125303 (2016).
[21] P. Agoston, K. Albe, R. M. Nleminen, and M. J. Puska, Phys. Rev. Lett. **103**, 245501 (2009).
[22] J. Vidal, S. Bott, P. Olsson, J.-F. Gulllemoles, and L. Relning, Phys. Rev. Lett. **104**, 056401 (2010).
[23] D. D. Richardson and J. Mahanty, J. Phys. C **10**, 397 (1977).
[24] G. Roman-Perez and J. M. Soler, Phy. Rev. Lett. **103**, 2009 (096102).
[25] F. D. Murnaghan, Proc. Nalt. Acad. Sci. USA **30**, 244 (1944).
[26] S. C. Abrahams and J. L. Bernstein, J. Chem. Phys. **59**, 5415 (1973).
[27] Y. Tomm and S. Fiechter, Journal of Ceramic Processing Research **6**, 141 (2005).
[28] L. Duran, C. Guerrero, E. Hernandez, J. M. Delgado, J. Contreras, S. M. Wasim, and C. A. Durante Rincon, J. Phys. and Chem. Solids **64**, 1907 (2003).
[29] C. Kim, G. Park, M. Jin, and D. Kim, Journal of the Korean Physical Society **48**, 951 (2006).
[30] S. C. Abrahams and J. L. Bernstein, J. Chem. Phys. **61**, 1140 (1974).
[31] S. M. Wasim, C. Rincon, G. Marin, and J. M. Delgado, Appl.Phys. Lett. **77(1)**, 94 (2000).
[32] R. R. Reddy, Y. Nazeer Ahammed, K. Rama Gopal, P. Abdul Azeem, T. V. R. Rao, and P. Mallikarjuna Reddy, Opt. Mater. **14**, 355 (2000).
[33] F. Birch, Phys. Rev. **71**, 1947 (809).
[34] Q. B. Meng, C. Y. Xiao, Z. J. Wu, F. Ke-an, Z. D. Lin, and S. Y. Zhang, Solid State Commun **107**, 369 (1998).
[35] R. Asokamani, R. M. Amirthakumari, R. Rita, and C. Ravi, Phys Status Solidi B **213**, 349 (1999).
[36] S. B. Zhang, S. H. Wei, and A. Zunger, Phys. Rev. Lett **78**, 4059 (1997).
[37] S. B. Zhang, S. H. Wei, A. Zunger, and H. Katayama-Yoshida, Phys. Rev. B **57**, 9645 (1998).
[38] W. Mones, *Electronic Properties of Semiconductors Interface* (Springer, Berlin, 2004).
[39] J. Tersoff, Phys. Rev. B **30**, 4874 (1984).
[40] C. S. Jiang, R. Noufi, K. Ramanathan, J. A. Abushama, H. R. Moutinho, and M. M. Al-gassim, Appl. Phys. Lett. **85**, 2625 (2004).
[41] J. E. Jaffe and A. Zunger, Phys. Rev. B **28**, 5822 (1983).
[42] M. Gajdos, K. Hummer, G. Kresse, J. Furthmuller, and F. Bechstedt, Phys. Rev. B **73**, 045112 (2006).
[43] S. Joshi, Ph.D. thesis entitled Structural, Electronic, and Optical Properties of Chalcopyrite Semiconductors (awarded in 2015).

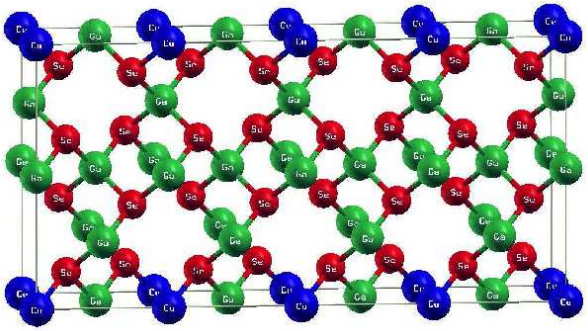

FIG. 1. Crystal structure of $CuGa_5Se_8$ with $(2V^{-}_{Cu}+Ga^{2+}_{Cu})$ defect pair.

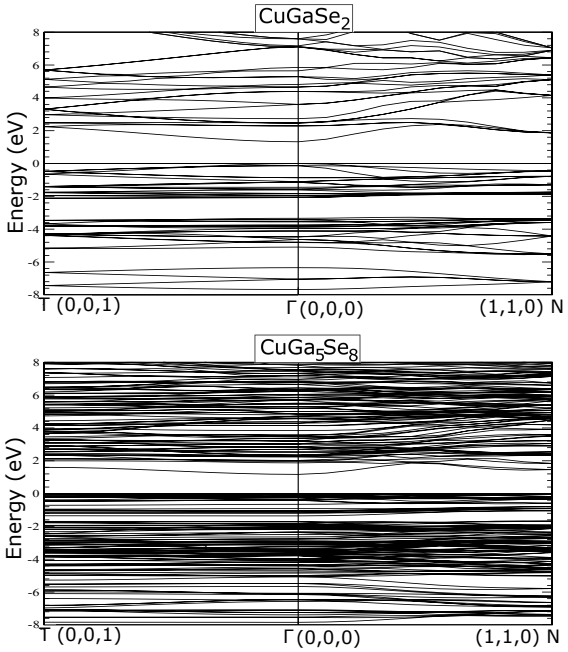

FIG. 2. Calculated band structure of $CuGaSe_2$ and $CuGa_5Se_8$ at T, Γ and N symmetry points.

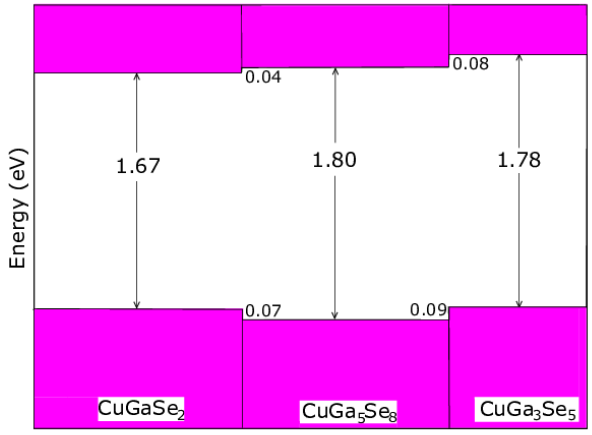

FIG. 3. Calculated band offsets (in eV) between $CuGaSe_2$, $CuGa_5Se_8$ and $CuGa_3Se_5$ ODCs.

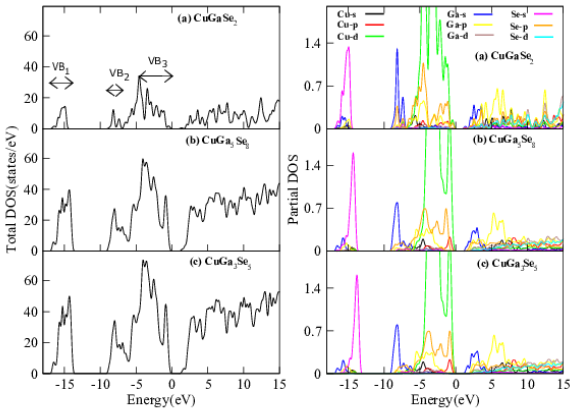

FIG. 4. Calculated total and partial density of states for $CuGaSe_2$, $CuGa_5Se_8$ and $CuGa_3Se_5$ are presented in panel (a-c) of Fig. 5a and Fig. 5b respectively.

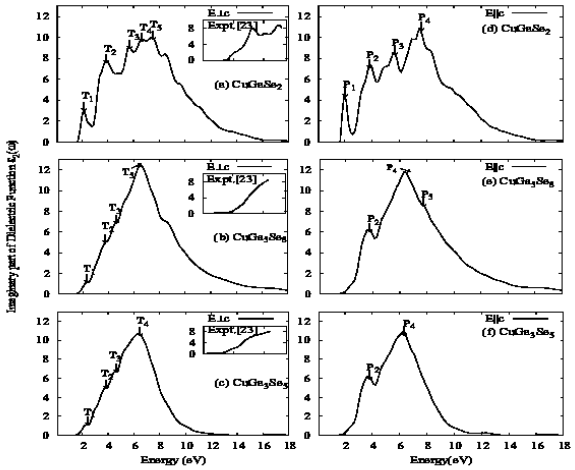

FIG. 5. Calculated imaginary part of dielectric function and corresponding measured data are presented in panel (a)-(f) for $CuGaSe_2$, $CuGa_5Se_8$ and $CuGa_3Se_5$ respectively.

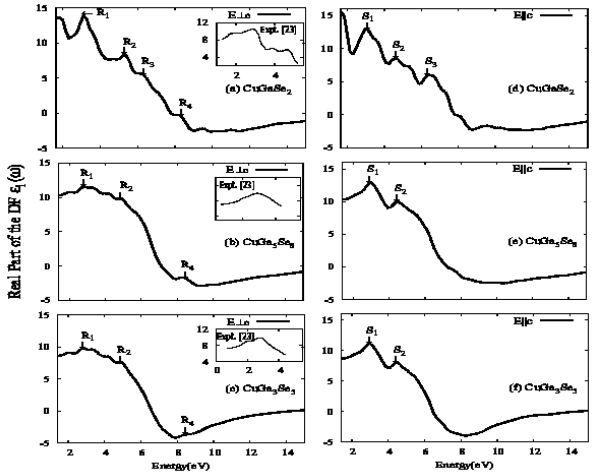

FIG. 6. Calculated real part of dielectric function and corresponding measured data are presented in panel (a)-(f) for $CuGaSe_2$, $CuGa_5Se_8$ and $CuGa_3Se_5$, respectively.